





## Article

# Sour Orange Microbiome Is Affected by Infections of *Plenodomus tracheiphilus* Causal Agent of Citrus Mal Secco Disease

Giulio Dimaria <sup>1,†</sup>, Alexandros Mosca <sup>2,†</sup> , Alice Anzalone <sup>1</sup>, Giuseppe Paradiso <sup>1</sup>, Daniele Nicotra <sup>1</sup> , Grete Francesca Privitera <sup>3</sup> , Alfredo Pulvirenti <sup>3</sup> and Vittoria Catara <sup>1,\*</sup> 

<sup>1</sup> Department of Agriculture, Food and Environment, University of Catania, 95123 Catania, Italy

<sup>2</sup> Department of Physics and Astronomy, University of Catania, 95123 Catania, Italy

<sup>3</sup> Department of Clinical and Experimental Medicine, University of Catania, 95123 Catania, Italy

\* Correspondence: vcatara@unict.it

† These authors contributed equally to this work.

**Abstract:** Mal secco is a severe vascular citrus disease (MSD) caused by the mitosporic fungus *Plenodomus tracheiphilus* (*Pt*). The pathogen enters through wounds on the above- and below-ground parts of the tree. The susceptible species sour orange (*Citrus aurantium*) is the most commonly used rootstock for lemon trees in Italy. In this study, sour orange seedlings were wound-inoculated with *P. tracheiphilus* in leaves or roots. Six months post-inoculation, the microbial communities of rhizosphere, endorhizosphere, and xylem endosphere samples from inoculated and healthy plants were analyzed by 16S rRNA and ITS (internal transcribed spacer) amplicon sequencing. The DNA of *Pt* was quantified by real-time PCR in the three compartments. According to our results, the endorhizosphere of root-inoculated plants showed the highest concentration of the pathogen DNA. Bacterial populations of potentially beneficial taxa (e.g., *Pseudomonas* and *Burkholderia*) were depleted in the rhizosphere of the inoculated plants. Infection through leaves and roots also produced a network-wide rewiring of microbial associations in sour orange roots. Overall, our findings revealed community-level changes induced by *Pt* infection in the sour orange root and xylem microbiome, providing further insights into the beneficial multispecies interactions in *Citrus*-associated microbial communities.

**Keywords:** *Citrus*; Mal secco; root microbiome; real-time PCR; amplicon-based metagenomics



**Citation:** Dimaria, G.; Mosca, A.; Anzalone, A.; Paradiso, G.; Nicotra, D.; Privitera, G.F.; Pulvirenti, A.; Catara, V. Sour Orange Microbiome Is Affected by Infections of *Plenodomus tracheiphilus* Causal Agent of Citrus Mal Secco Disease.

*Agronomy* **2023**, *13*, 654. <https://doi.org/10.3390/agronomy13030654>

Academic Editor: Yueqiang Zhang

Received: 2 February 2023

Revised: 18 February 2023

Accepted: 21 February 2023

Published: 24 February 2023



**Copyright:** © 2023 by the authors. Licensee MDPI, Basel, Switzerland. This article is an open access article distributed under the terms and conditions of the Creative Commons Attribution (CC BY) license (<https://creativecommons.org/licenses/by/4.0/>).

## 1. Introduction

Lemon (*Citrus limon*) is the third most important species within the genus *Citrus*, with a global production, together with limes, amounting to 20.5 million t [1]. The Mediterranean Basin accounts for approximately half of the global lemon production. Turkey is the major producing country (950,000 t per year), followed by Spain (884,900 t) and Italy (446,000 t) [1]. Many countries of the Mediterranean Basin are affected by Mal secco disease (MSD), a detrimental tracheomycosis caused by the mitosporic fungus *Plenodomus tracheiphilus* (Petri) Gruyter, Aveskamp and Verkley (formerly: *Phoma tracheiphila* (Petri) Kantschaveli and Gikashvili) [2]. Although several genera in the Rutaceae, such as *Citrus*, *Poncirus*, *Severinia*, and their hybrids, can serve as hosts, the disease is a major constraint for successful lemon (*C. limon*) production in the areas where the fungal pathogen is present [3–5]. Morocco and Portugal, while still free of MSD, have suitable conditions for its development [6].

Up to the 1950s, MSD destroyed no less than 12,000 hectares of lemon groves in Sicily and 20,000 lemon plants in Mersin Province, Turkey [4]. The average annual yield loss was 12.3% in Turkey and 50–60% in Greece [4]. In the last 30 years, the lemon growing area and production in Sicily have decreased by 45% and 41%, respectively [5].

*P. tracheiphilus* is included on the A2 quarantine pest lists of the European and Mediterranean Plant Protection Organization (EPPO), and the A1 lists of several global regional plant protection organizations. According to the Plant Health panel of EFSA, *P. tracheiphilus* has been classified as a regulated non-quarantine pathogen in Europe [2].

As for tracheomycotic diseases, the distribution and severity of MSD symptoms depend on xylem colonization [4,7]. Two non-selective phytotoxic glycoproteins of 93 kDa and 60 kDa (called Pt60) extracted from culture filtrates of *P. tracheiphilus* were found to reproduce symptoms of leaf vein chlorosis when injected into citrus leaves [3]. The highest incidence of epigeal infections is usually observed after meteoric events which cause wounds and abscission of leaves or bark as well as xylem lesions on twigs and stems [4]. Root infections have been characterized by a chronic, slow occurring disease called “Mal nero” (black disease) and a sudden death syndrome called “Mal fulminante” [4]. During colonization, fungal hyphae develop intercellularly since they reach the xylem and spread progressively [8]. Host gums, mycelium, and debris of cell wall fungal degradation contribute to xylem vessel clogging [4], leading to the impairment of water transport [9]. Inoculum is provided by spores released by pycnidia differentiated on withered bark tissue of infected organs or by phialides formed on hyphae that can develop on cut wood surfaces, wounded tissues, and even within xylem from pruning residues lying on the ground [3,4].

The composition and function of the citrus microbiome have stimulated significant research aimed at better understanding the microbial interactions and tackling citriculture challenges through citrus microbiome engineering [10–12]. The evolution of the plant “holobiont”, comprising the host plant and its microbiota, has led to variations in both the host genome and its microbiome [13–15]. The plethora of microorganisms that live in close association with multiple plant microhabitats in different organs may induce beneficial, neutral, or adverse effects [13,16].

An increasing number of studies have been undertaken on the potential functions of individual microorganisms and communities or entire natural niches now that culture-independent high-throughput sequencing methods have been developed [17,18]. Great attention has been devoted to the microbiome of the plant root environment, analyzing functions and traits related to plant growth, development, and health in several plant hosts [19,20]. These communities benefit from the acquisition of nutrients, and stress tolerance, and protect the plants against soil-borne pathogens [16,21].

Citrus-associated microbiome studies on different compartments (soil, root, leaves, phloem, seeds) from several *Citrus* species and cultivars have been undertaken [12,22] also with the aim to select potentially host-beneficial microbes [23,24]. The study of microorganisms commonly found within citrus rhizosphere microbiomes and their functional traits has highlighted that the core members of this plant compartment are tightly and stably associated with citrus hosts from different global geographical locations [11]. The citrus microbiome has been investigated by metagenomics only in a few pathosystems. The leaf microbiome has been investigated in citrus plants affected by melanose disease caused by *Diaporthe citri* [25] or to explore the etiology of complex syndromes such as Citrus Decline Disease (CDD) [26] and the leaf fungal disease Citrus Greasy Spot (CGS) [27]. The citrus rhizosphere microbiome has been explored in grapefruit (*C. paradisi*) trees affected by foot rot grafted on sour orange (*C. aurantium*) [28] and extensively investigated in Huanglongbing (HLB)-affected plants [29–34].

Citrus foot rot by *Phytophthora* spp. has been associated with a depletion in beneficial bacteria and fungi in the endorhizosphere of symptomatic trees compared to healthy ones [28]. ‘*Candidatus Liberibacter asiaticus*’ (CLAs), one of the fastidious phloematic bacteria associated with HLB, affects the structure and composition of the bacterial community associated with citrus leaves [26,30,35] and roots [29,30,32–34,36]. In addition, the bacterial community composition of both citrus roots and endosphere of all above-ground tissues has been proven to vary due to the application of biofertilizers [37], antibiotics [38–40], and thermotherapy treatments [39] for HLB disease control. A pivotal role in the decline

and death of HLB-affected plants was attributed to changes in root microbial communities, leading to a severe dysbiosis status [33].

To the best of our knowledge, no metagenomic studies have been carried out on citrus xylem dwellers. However, the effects of Citrus Variegated Chlorosis (CVC) associated with the xylem-limited bacterium *Xylella fastidiosa* on citrus microbial communities, which was investigated by a culturable approach and DGGE (Denaturing Gradient Gel Electrophoresis), highlighted that infections induce differences in the endophytic culturable bacteria of leaves and branches of sweet orange (*C. sinensis*) and mandarin (*C. reticulata*) plants [41].

To date, the influence of MSD caused by *P. tracheiphilus* on the microbial communities of citrus roots and xylem has never been explored. This study investigates whether Mal secco infections affect the microbial composition and community structure at the rhizosphere and endosphere levels by an amplicon-based (16S rRNA and ITS sequences) metagenomic approach. As the main microbial interactions in the soil depend on the roots, the trials were performed on *Pt*-inoculated seedlings of sour orange, which is the most popular rootstock for lemons in Italy and has been extensively used in studies on *P. tracheiphilus*-*Citrus* pathosystem [4,5]. Our results provide new insights for the development of sustainable strategies aimed at controlling MSD.

## 2. Materials and Methods

### 2.1. Fungal Isolates and Culture Conditions

*P. tracheiphilus* PVCT Pt57, a virulent isolate from *Citrus limon* plants affected by Mal secco [42,43], was routinely grown at  $23\text{ }^{\circ}\text{C} \pm 2$  on potato dextrose agar (PDA, Oxoid, Milan, Italy) or carrot agar (CA) [44].

*P. tracheiphilus* phialoconidia were obtained in carrot broth (300 g of carrots·L<sup>-1</sup>), as described by Salerno and Catara [45], with minor modifications (incubation at 22 °C instead of 20 °C). Phialoconidia were counted using a hemacytometer and diluted up to 10<sup>6</sup> mL<sup>-1</sup> with sterile distilled water (SDW) for the leaf- and root-inoculation assays.

### 2.2. Plant Materials

Four-month-old *Citrus aurantium* (sour orange) seedlings in pots (20 cm diameter) filled with a commercial virgin peat-based substrate were leaf-inoculated and root-inoculated (ten seedlings per inoculation method) with *P. tracheiphilus* PVCT Pt57 and grown in an unheated greenhouse. Control plants were only treated with SDW. For both inoculation methods, the inoculum consisted of 10<sup>6</sup> conidia·mL<sup>-1</sup> aqueous suspension of the fungus phialoconidia. Leaf-inoculations were performed by placing 10 µL of conidial suspension on the secondary veins of young and fully expanded leaves [43]. Slight wounds were then made on the leaves at the suspension drops by gently pressing with three entomological needles. For each seedling, four leaves were inoculated at four points. For root inoculations, after uprooting the plants, the root tips were cut, and the roots were immersed in the inoculum suspension for 10–15 min. Plants were finally placed into the same peat-filled pot. The leaf and root infection symptoms were monitored weekly and evaluated using the empirical scales proposed by Luisi et al. [46] and Scaramuzzi et al. [47], respectively.

### 2.3. Sample Processing

Six months after inoculation (leaf-inoculation, root-inoculation, and uninoculated control), three compartments were analyzed: the rhizosphere, endorhizosphere, and xylem endosphere. Composite rhizosphere samples were obtained by processing together the rhizospheres of three randomly selected *Citrus aurantium* seedlings. The same sampling method was used for the endorhizosphere and xylem endosphere samples. Three composite samples for each compartment and treatment were considered.

Root samples were processed according to Anzalone et al. [48,49], with minor modifications. Rhizosphere samples were obtained by gently shaking the roots to remove the non-adhering soil. Roots were then transferred into sterile 50 mL centrifuge tubes containing 25% *w/v* sterile phosphate saline buffer (PBS: NaCl 137 mM, KCl 2.7 mM,

$\text{Na}_2\text{HPO}_4$  10 mM,  $\text{KH}_2\text{PO}_4$  1.8 mM, pH 7.4) and mixed thoroughly by vortexing for 2 min. Endorhizosphere samples were obtained by surface sterilizing the roots which were first submerged in 75% ethanol solution (2 min), followed by 50% sodium hypochlorite solution (2 min), and ethanol 75% (1 min), and rinsed five times in SDW. In order to verify the surface sterility of the samples, sterilized roots were placed on PDA at  $27\text{ }^\circ\text{C} \pm 2$  for 7 days. The lack of bacterial and fungal growth confirmed the sterility of the root surfaces.

To obtain the xylem endosphere samples, after removing the leaves, stems were surface-sterilized by immersion as described above. The bark was peeled off. The surface sterility of xylem samples was verified as described for the endorhizosphere samples. Endorhizosphere and xylem samples were homogenized separately with a mortar and pestle and suspended in 25% *w/v* sterile PBS [49]. The rhizosphere samples and the endorhizosphere and xylem homogenates were aliquoted into 2-mL reaction tubes and centrifuged at 13,000 rpm and  $4\text{ }^\circ\text{C}$  for 30 min. Pellets were then stored at  $-80\text{ }^\circ\text{C}$  for further processing.

#### 2.4. Total DNA Extraction and Quantitative Detection of *P. tracheiphilus*

Total genomic DNA was extracted with DNeasy PowerSoil Pro Kit (Qiagen, Hilden, Germany), according to the manufacturer's instructions. DNA concentration and quality were determined with a NanoDrop 1000 spectrophotometer (Thermo Scientific, Wilmington, DE, USA). Detection and quantification of *P. tracheiphilus* DNA in root- and leaf-inoculated seedlings were performed according to a species-specific real-time PCR protocol [50,51]. Amplification was carried out with GR70 and GL1 primers targeting an 84-pb DNA segment of *P. tracheiphilus* DNA, and the dual-labeled fluorogenic probe PP1 [50,51]. Real-time PCR assays were performed using the QuantiNova Probe PCR Kit (Qiagen, Hilden, Germany), 400 nM of each primer, 200 nM probe, and 1  $\mu\text{L}$  of target DNA. All reactions included a blank, replacing DNA with ultrapure water, and positive controls (serial dilutions of *P. tracheiphilus* PVCT Pt57 DNA). The real-time PCR program consisted of an initial denaturation step at  $95\text{ }^\circ\text{C}$  for 2 min, followed by 40 cycles of 10 s at  $95\text{ }^\circ\text{C}$ , 15 s at  $62\text{ }^\circ\text{C}$ , and 15 s at  $72\text{ }^\circ\text{C}$ . All real-time PCR reactions were performed in a Bio-Rad (Bio-Rad, Hercules, CA, USA) iQ5 Cyclo real-time PCR detection system.

The standard curve for fungal DNA quantification was constructed using *P. tracheiphilus* PVCT Pt57 isolate DNA (100 ng/ $\mu\text{L}$ ) serially diluted in SDW by plotting Ct (cycle threshold) values versus the logarithm-transformed DNA concentration values of each ten-fold dilution series.

#### 2.5. Library Preparation and Amplicon Sequencing

Library preparation and amplicon sequencing were conducted at IGA Technology Services (Udine, Italy). For bacterial community profiling, the V3–V4 hypervariable region of the bacterial 16S rRNA gene was amplified with primers 16S-341F and 16S-805R [52]. Peptide nucleic acid (PNA)-clamping was applied during the first 16S rRNA amplification step to block amplification of host chloroplast and mitochondrial 16S rRNA gene sequences. For fungal community profiling, primers ITS1 and ITS2 [53] were used to amplify part of the ITS1 region of the fungal rRNA operon. The 16S and ITS libraries were sequenced on an Illumina MiSeq instrument (Illumina, San Diego, CA, USA) in paired-end 300-bp mode reads whose ends were overlapped to generate high-quality full-length sequences and ensure accurate taxonomic classification.

#### 2.6. Bioinformatics and Statistical Analysis

According to Illumina indexing system, 16S and ITS raw Illumina FASTQ files were demultiplexed and quality checked by FastQC [54]. Following the QIIME 2 pipelines [55], the USEARCH algorithm (version 8.1.1756) was used for chimera filtering, grouping of replicate sequences, sorting sequences per decreasing abundance, and OTU (operational taxonomic unit) identification and then summarized in feature tables.

The most abundant 16S reads in each OTU were selected as representative sequences and extracted, aligned, and assigned taxonomically using the RDP classifier classification from the RDP database [56] trained to the Greengenes 16S rRNA gene database version 2013\_8 (confidence threshold  $\geq 0.5$ ) [57]. The UNITE ITS database was used for the fungal ITS region (version 8.1) [58]. Alpha and beta diversity, based on the OTU tables for the bacterial and fungal communities, were evaluated for each treatment (control, leaf-inoculation, root-inoculation) and compartment (rhizosphere, endorhizosphere, xylem) using the phyloseq package in R (version 4.0.2) [59,60].

Statistical significance was analyzed using the Kruskal–Wallis test for alpha diversity and the two-sided Student two-sample *t*-test for beta diversity. Differential abundance analysis was performed with DESeq2 [61] to detect the enriched and depleted bacterial and fungal genera between the controls and inoculated samples of the same compartment. Bacterial and fungal networks were constructed for each treatment (control, leaf-inoculation, and root-inoculation), including the rhizosphere, endorhizosphere, and xylem compartments in each network. The most abundant bacterial and fungal genera were used for the construction of co-occurrence networks. MENAP was used [62] following the developer's recommendations, choosing the greedy modularity as separation method, and represented in Cytoscape [63]. Differential network analysis was performed between the networks of the control samples and those of the inoculated samples using the Diffany framework [64] in Cytoscape.

### 2.7. *Plenodomus* Sequence Analysis

For sequence analysis, partial ITS1 sequences of the OTUs identified as *Plenodomus* sp. were searched against the National Center for Biotechnology Information (NCBI) nucleotide database using Basic Local Alignment Search Tool BLASTN (<https://www.ncbi.nlm.nih.gov/>, accessed on 14 November 2022). Only sequences with the highest similarity were considered for the taxonomic assignment. For phylogenetic analysis, sequences of *Plenodomus* sp. OTUs and partial ITS1 of representative Pleosporales were aligned using MUSCLE in MEGA X [65]. A cladogram was constructed by using the maximum likelihood method and Kimura 2-parameter model [66]. The analysis was performed with 1000 bootstrap replications.

## 3. Results

### 3.1. Quantification of *Plenodomus tracheiphilus* in Sour Orange Seedlings

*P. tracheiphilus* infections in leaf- and root-inoculated sour orange seedlings simulating canopy and below-ground infections that occur via wounds were monitored visually over time and six months after inoculation using quantitative real-time PCR. Upon leaf-inoculation, the first symptoms appeared 7 dpi (days post-inoculation) on a small number of infected sites (10%). At the last recording date (35 dpi), 90% of sites were symptomatic and the leaves showed typical citrus MSD symptoms consisting of chlorosis extending up to the leaf margin. Two months post-inoculation, leaf-inoculated seedlings showed defoliation. In the remaining leaves, chlorosis of the entire leaf was observed (Figure 1A).

Most of the root-inoculated seedlings showed stunted growth compared to the non-inoculated controls. Mild chlorosis of the midribs of newly formed leaves was observed six months post-inoculation (Figure 1B). The remaining plants were asymptomatic. For both inoculated plants (through leaves or roots), no secondary symptoms were observed.

Six months post-inoculation, total genomic DNA was extracted from the rhizosphere, endorhizosphere and xylem endosphere samples. *P. tracheiphilus* DNA was quantified by a species-specific real-time PCR assay (Supplementary Table S1). Based on a standard curve for absolute quantification obtained with serial dilution of the DNA of *P. tracheiphilus* isolate PVCT Pt57 (the same one used for the inoculations), the amount of DNA per gram of sample was estimated, with a quantification limit of 0.1 pg (data not shown).

Regarding the leaf-inoculated plants, the fungus was only detected in the xylem with DNA concentrations from 8.8 to 58.3 pg·g of tissue<sup>-1</sup>. No amplification signal was

detected from the rhizosphere and endorhizosphere samples of leaf-inoculated seedlings. In contrast, *P. tracheiphilus* was detected in all samples from root-inoculated seedlings. Variable concentrations of the pathogen DNA, namely 5.3–205.0, 32.6–34,862.2 and 5.5–56.2 pg·g of tissue<sup>-1</sup> were detected in the rhizosphere, endorhizosphere, and xylem endosphere samples, respectively.



**Figure 1.** Symptoms developed upon *Plenodomus tracheiphilus* inoculation in roots (A) and leaves (B) of sour orange seedlings six and two months post-inoculation, respectively, and non-inoculated control (C).

### 3.2. Assembly Patterns of Healthy and Diseased Sour Orange Seedlings

#### 3.2.1. Alpha and Beta Diversity

Bacterial and fungal communities were obtained from the rhizosphere, endorhizosphere, and xylem of *C. aurantium* (sour orange) seedlings colonized by *P. tracheiphilus* upon artificial inoculation either on the leaves or roots and from the uninoculated plants. A total of 552,234 and 514,565 reads (for the bacterial and fungal communities, respectively), were obtained after quality filtering (length trimming, denoising, and exclusion of chimeric sequences). For 16S rRNA, a total of 551,069 reads were recovered after the removal of chloroplast and mitochondrial reads. Distributions of 6651, 5038, and 1556 of the total OTUs were recovered for the rhizosphere, endorhizosphere, and xylem samples, respectively. For ITS1, a total of 514,565 reads were recovered after the removal of host sequence reads. Distributions of 791, 181, and 213 of the total OTUs were recovered for the rhizosphere, endorhizosphere, and xylem samples, respectively.

The bacterial alpha diversity, estimated by Chao1 richness and Shannon diversity indices, was significantly different ( $p < 0.05$ ) among all three compartments. The highest values were observed in the rhizosphere which decreased from the endorhizosphere to the xylem (Supplementary Figure S1A,B). No significant differences in alpha diversity indices were detected when comparing the uninoculated control samples versus those inoculated with *P. tracheiphilus*, although a slight reduction was observed in the rhizosphere of inoculated plants (Supplementary Figure S1A,B). The fungal communities of some of the different sample groups showed significant differences either in richness (rhizosphere vs. endorhizosphere and xylem) or diversity (rhizosphere and endorhizosphere vs xylem) (Supplementary Figure S1C,D). In the endorhizosphere of plants inoculated with the pathogen via roots, a reduction in both richness and diversity was observed. The high concentration of *P. tracheiphilus*, as ascertained by real-time PCR, led to a reduction in other fungal taxa, also reducing the evenness and therefore diversity. Fungal communities of the rhizosphere of the same samples showed an increased richness and reduced diversity.

The PCoA for the beta diversity of the bacterial community based on Bray–Curtis dissimilarity distances showed a significant division between the compartments ( $p = 0.001$ ) (Supplementary Figure S2A) but no effect was observed upon *P. tracheiphilus* inoculation. The beta diversity analysis of fungal communities highlighted the dispersion of root-inoculated rhizosphere and endorhizosphere samples (Supplementary Figure S2B).

### 3.2.2. Relative Abundance of Bacterial Communities

At the phylum level, the most represented bacterial communities in the rhizosphere of control sour orange seedlings were Proteobacteria (26.3%), Firmicutes (14.2%), and Planctomycetes (13.7%), followed by Verrucomicrobia (6.3%) and Bacteroidetes (6.9%); a large group of other bacteria (16.4%) was also observed (Figure 2A). Endophytic bacterial communities both of the root and xylem of control plants were dominated by Firmicutes (46.3 and 49.8%, respectively), and Proteobacteria (29.5 and 25.3%, respectively). Other phyla, more represented in the endorhizosphere than the xylem, were Actinobacteria, Bacteroidetes, and Planctomycetes. Only minor changes were observed at the phylum level in bacterial communities of the *P. tracheiphilus* inoculated as compared to non-inoculated seedlings. At the bacterial phylum level, Actinobacteria (8.2%) and Bacteroidetes (4.7%) were more abundant in the endorhizosphere of leaf-inoculated plants (4.8 and 2.4 in control plants, respectively). Bacteroidetes were also more abundant in the endorhizosphere of root-inoculated plants (7.7% vs. 2.4% in control plants). Firmicutes decreased in the endorhizosphere of root-inoculated plants (34.5% vs. 46.3% in control plants). Actinobacteria also increased in the xylem of root-inoculated plants (3.4% vs. 1.9% in control plants, respectively).

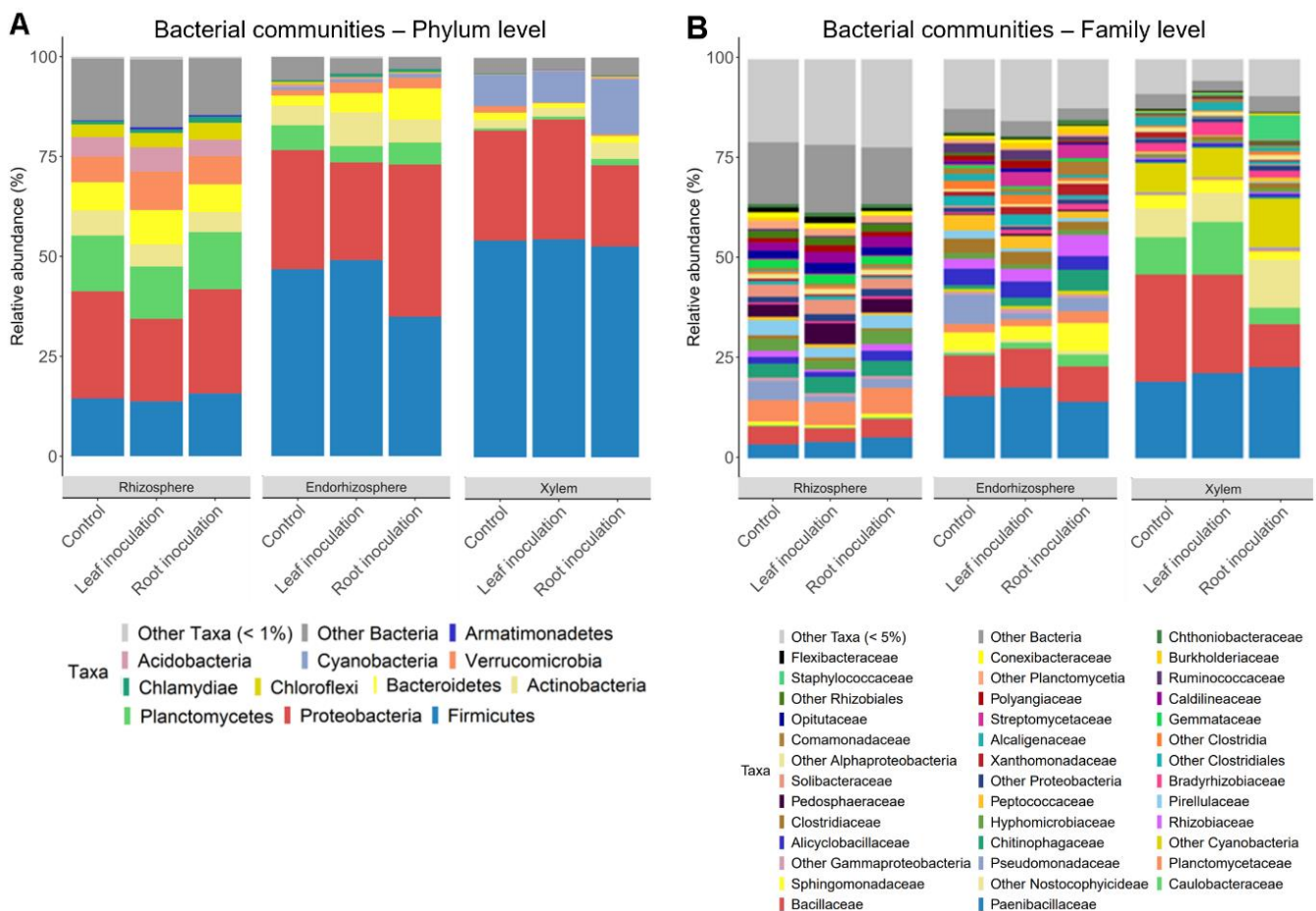


**Figure 2.** Relative abundances of the bacterial communities at the phylum (A) and family (B) taxonomic levels in the rhizosphere, endorhizosphere, and xylem compartments of control (non-inoculated) and inoculated (through leaves or roots) sour orange seedlings. Bacterial phyla and family taxa less abundant than 1% and 5%, respectively, are reported as “Other Taxa”.

The analysis of the relative abundance at the family level was investigated in order to assess the effect of inoculation with *P. tracheiphilus* on the sour orange microbiome. In the rhizosphere samples of control plants, the most relatively abundant bacterial taxa were Planctomycetaceae (5.2%), Pseudomonadaceae (4.7%), Bacillaceae (4.6%), Pirellulaceae

(3.6%), and unidentified bacteria (15.8%) (Figure 2B). A decrease in Pseudomonadaceae was observed in plants inoculated either via roots (1.4%) or leaves (2.1%) than in control plants (4.7%). Bacterial root endophytic communities of control plants were characterized, at the family level, by a higher relative abundance in Paenibacillaceae (15.6%) and Bacillaceae (10.2%), than those observed in the rhizosphere, which together totaled 48% in the xylem of control plants. As in the rhizosphere, in the endorhizosphere Pseudomonadaceae were reduced in *P. tracheiphilus* inoculated plants irrespectively of the inoculation site (1.5%, 3.3%, and 7.3% for leaf-, root- and non-inoculated plants). The families Sphingomonadaceae, Rhizobiaceae, and Chitinophagaceae were detected at a higher relative abundance in root-inoculated samples (7.0 vs. 4.4%, 5.3 vs. 2.4% and 5.3 vs. 0.9%, in control plants, respectively), while Paenibacillaceae and Clostridiaceae were less present in the same samples (15.6% vs. 14.3% and 3.6% vs. 2.0% in control plants, respectively).

The family Staphylococcaceae was detected at a higher relative abundance in the xylems of root-inoculated plants (7% vs. 0.4 and 0.5 % in leaf-inoculated and in control plants, respectively), while Bacillaceae and Caulobacteraceae were less represented in the same samples (12.1% vs. 28.8% and 4.6% vs. 10.0% in control plants, respectively). Other Nostocophycidae and Sphingomonadaceae were more abundant in root-inoculated plants (13.6% vs. 7.7% and 2.3% vs. 3.5% in control samples, respectively).

### 3.2.3. Relative Abundance of Fungal Communities

At the phylum level, fungal communities of control plants were dominated by Ascomycota in all analyzed compartments (81%, 95%, and 55% in all analyzed samples of the rhizosphere, endorhizosphere, and xylem compartments, respectively). Basidiomycota were increased in the xylem environment. Other represented phyla were Zygomycota and Rozellomycota.

At the fungal phylum level, Ascomycota increased in the rhizosphere of root-inoculated plants (97% vs. 81% in control plants, respectively), while Rozellomycota decreased (1.7% vs. 4.8% in control plants, respectively) (Figure 3A). Basidiomycota and Rozellomycota increased in the endorhizosphere of leaf-inoculated plants compared to control plants (7.2% vs. 3.2% and 1.6% vs. 0.3%, respectively). Zygomycota decreased in the endorhizosphere of root-inoculated plants (0.03% vs. 0.8% in control plants, respectively), and in the xylem of leaf-inoculated plants (3.4% vs. 6.6% in control plants, respectively).

Fungal community analysis at the family level showed a higher relative abundance of Trichocomaceae, which is the most abundant taxon in the rhizosphere, in *P. tracheiphilus* root- and leaf-inoculated samples (71% and 34%, respectively), than in control plants (25%) (Figure 3B). In the rhizosphere, Annulatasceae were detected at a higher relative abundance in the rhizospheres of root-inoculated plants (2% vs. 0%, in control plants, respectively). In contrast, the abundance of Davidiellaceae and Rhizopodaceae (10% vs. 1%, in control plants, respectively), and Rozellomycota (5% vs. 2% in control plants, respectively), was lower in the rhizosphere of root-inoculated plants than in control plants.

In the endorhizosphere of leaf-inoculated plants, Orbiliaceae (45% vs. 18% in control plants, respectively), were detected at a higher relative abundance, whereas Nectriaceae (5% vs. 1%, in control plants, respectively), showed a lower abundance in both inoculated samples. In the xylems, the fungal family with the highest relative abundance was Trichocomaceae (10%), in both root-inoculated and control plants. In addition, in the xylems of the root-inoculated samples, Mortierelliaceae (8% vs. 6% and 3% in leaf-inoculated and control samples, respectively), and Leptosphaeriaceae were more abundant (4% vs. 1% and 0% % in leaf-inoculated and control samples, respectively).

Leptosphaeriaceae (the family to which *P. tracheiphilus* belongs) was the most abundant taxon (58%) in the endorhizosphere of the root-inoculated seedlings. It was also detected, although to a lower extent, in the rhizosphere of root-inoculated plants (0.03%) and in the xylem of leaf- (1%) and root-inoculated plants (4%). Three OTUs, namely SH207506.07FU\_JF740253\_refs (235 bp), New.ReferenceOTU456 (234 bp), and New.CleanUp.ReferenceOTU22126 (251 bp) of the fungal community were identified as *P. chrysanthemi*, ac-



according to the UNITE ITS database. SH207506.07FU\_JF740253\_refs OTU (total of 9673 reads) was detected both in the rhizosphere, endorhizosphere, and xylem of root-inoculated plants and in the xylem of leaf-inoculated plants. BLASTN analysis resulted in 100% identity with *P. tracheiphilus* strain IS3\_15 (MK461058.1) and *P. chrysanthemi* strain ISR2\_3 (MK460988.1) and with isolate PVCT Pt57 (data not shown). The other two OTUs were instead represented by a total of two reads each in the endorhizosphere of root-inoculated samples and showed an identity of 96.5% and 98.3% with the above-mentioned GenBank accessions and the *P. tracheiphilus* isolate used in this study.

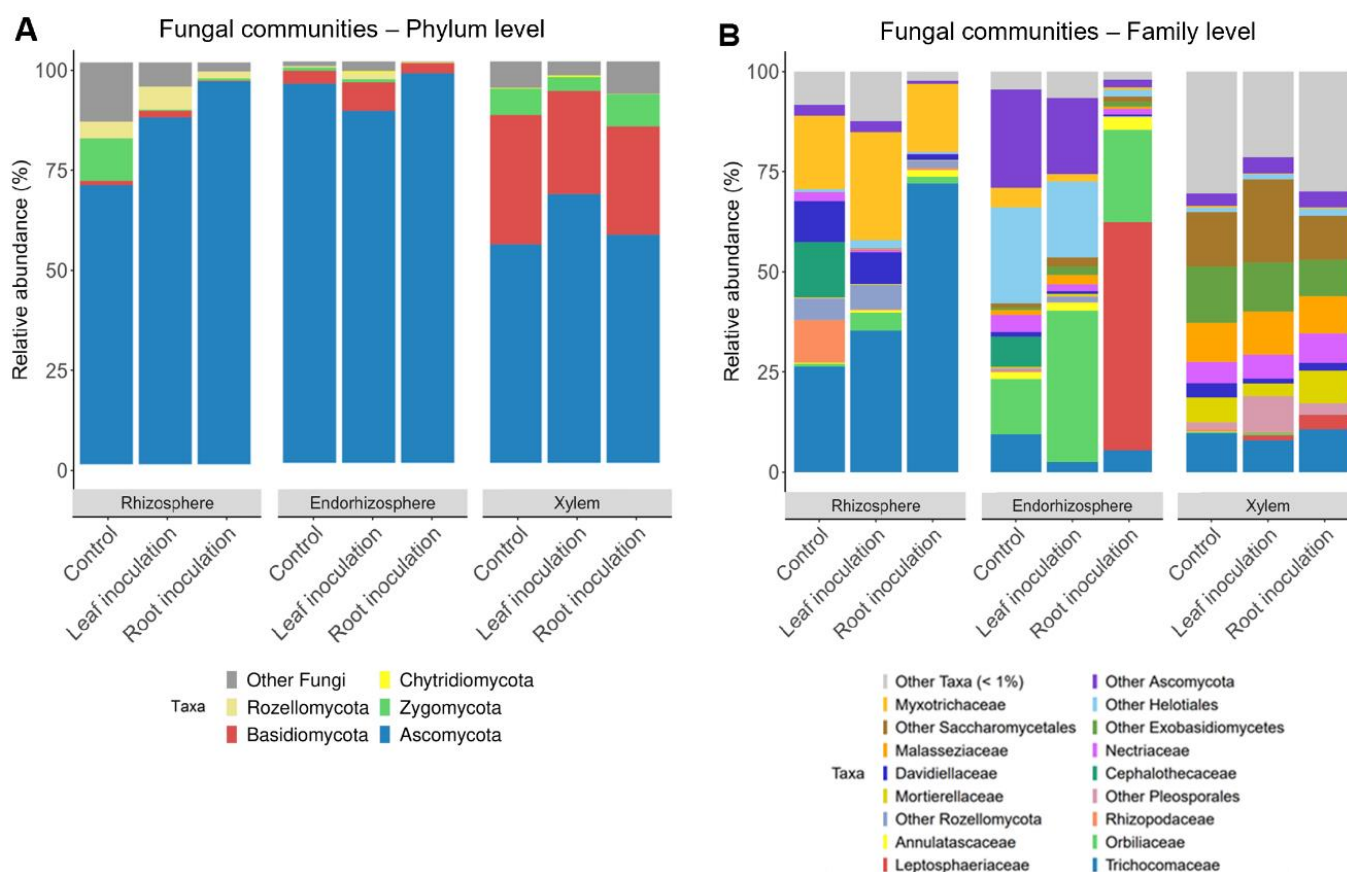


**Figure 3.** Relative abundances of the fungal communities at the phylum (A) and family (B) taxonomic levels in the rhizosphere, endorhizosphere, and xylem compartments of control (non-inoculated) and inoculated (through leaves or roots) sour orange seedlings. Fungal family taxa less abundant than 1% are reported as “Other Taxa”.

A cladogram based on the partial ITS1 gene sequences of representative *Plenodomus* sp. isolates and other closely related taxa showed that all three OTUs cluster within a phylogroup including both *P. tracheiphilus* and *P. chrysanthemi* strains (Supplementary Figure S3).

#### 3.2.4. Exploring Differentially Abundant Bacterial and Fungal Genera in Inoculated Plants

Differentially abundant bacterial and fungal genera were evaluated for each compartment comparing the sour orange seedlings inoculated with *P. tracheiphilus* by leaf- and root-inoculation and non-inoculated seedlings. The differential abundances of the genera that were statistically significant ( $p < 0.05$ ) in at least in one of the pairwise comparisons are shown in Figure 4A. In the rhizosphere, 27 and 14 bacterial genera differed significantly when comparing leaf-inoculated (LE) and root-inoculated (RE) to non-inoculated plants, whereas in the endorhizosphere, 25 and 19 bacterial genera differed significantly compared to LE and RE, respectively (Figure 4A).

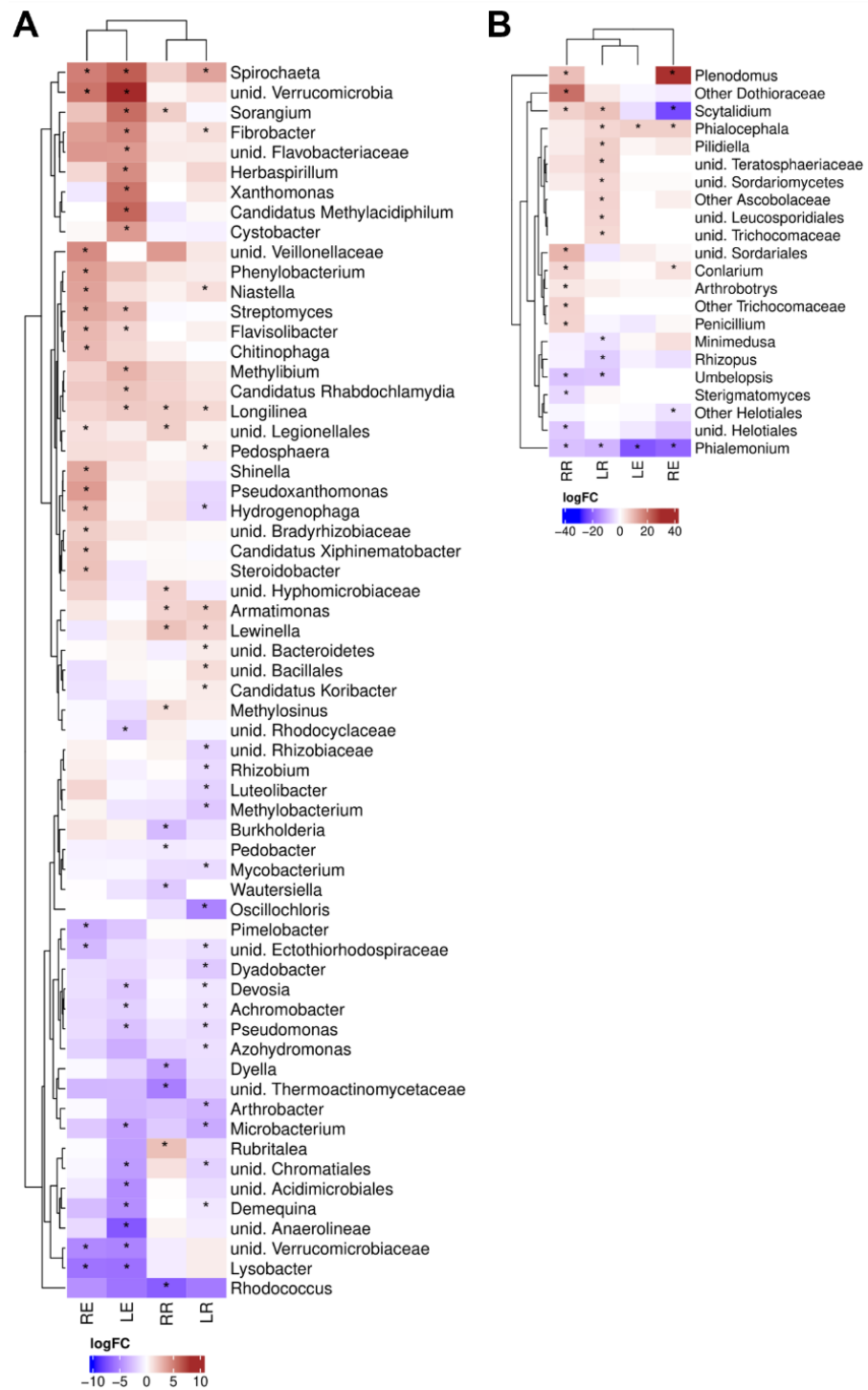


**Figure 4.** Bacterial (A) and fungal (B) heatmap of differentially abundant taxa present in the rhizosphere (LR) and endorhizosphere (LE) samples of the leaf-inoculated seedlings and in the rhizosphere (RR) and endorhizosphere (RE) samples of root-inoculated seedlings. Differentially abundant taxa were evaluated among the most significant samples (\* indicates  $p < 0.05$ ). Each cell depicts the  $\log_2$  fold change ( $\logFC$ ) of each microbial taxon and is colored according to depleted (blue), not differentiated (white), and enriched (red) conditions.

Regarding the rhizosphere, bacterial genera *Longilinea*, *Armatimonas*, and *Lewinella* were enriched both in the leaf- and root-inoculated sour orange seedlings compared to the non-inoculated seedlings ( $p < 0.05$ ) (Supplementary Tables S2 and S3). The following genera

were enriched after infection through either leaves or roots: *Spirochaeta*, *Fibrobacter*, *Niastella*, *Longilinea*, and *Pedosphaera*, and *Sorangium*, *Armatimonas* and *Methylosinus*, respectively ( $p < 0.05$ ) (Figure 4A). In contrast, no significant bacterial genera were found to be depleted in either sample type, although the heatmap indicates a tendency in that direction for some families. Several genera, namely *Microbacterium*, *Arthrobacter*, *Azohydromonas*, *Pseudomonas*, *Achromobacter*, *Devosia*, *Dyadobacter*, *Oscillochloris*, *Methylobacterium*, *Luteolibacter*, *Rhizobium*, and *Hydrogenophaga* were depleted in the leaf-inoculated seedlings, whereas in those inoculated via the roots only *Rhodococcus*, *Dyella*, *Wautersiella*, *Pedobacter*, *Burkholderia* were depleted.

Concerning the endorhizosphere, *Streptomyces*, *Flavisolibacter*, and *Spirochaeta* were significantly enriched in both the root- and the leaf-inoculated samples, whereas a depletion of the genus *Lysobacter* was observed (Supplementary Tables S4 and S5).

In leaf-inoculated samples, genera *Fibrobacter*, *Herbaspirillum*, *Xanthomonas*, *Methylobacterium*, *Cystobacter*, *Methylobacterium*, 'Candidatus Rhabdochlamydia' were significantly enriched, whereas genera *Devosia*, *Achromobacter*, *Pseudomonas*, *Microbacterium*, and *Demiquina* were significantly less abundant than in the control seedlings. Considering the root-inoculated samples, the enriched genera in the endorhizosphere were *Phenyllobacterium*, *Niastella*, *Chitinophaga*, *Shinella*, *Pseudoxanthomonas*, 'Candidatus Xiphinematobacter', and *Steroidobacter*, whereas only genus *Pimelobacter* was depleted.

In xylem, no significantly enriched or depleted genera were shared between the treatments. *Hydrogenophaga*, *Peptoniphilus*, and *Finegoldia* were enriched in the leaf-inoculated plants, while *Staphylococcus* was the only bacterial genus enriched after the root-inoculation (Supplementary Table S6). *Ochrobactrum* and *Ramlibacter* were depleted in the leaf-inoculated plants (Supplementary Table S7).

Differential abundance analysis highlighted a statistically significant depletion in *Pseudomonas* in the endorhizosphere and rhizosphere of sour orange seedlings inoculated with *P. tracheiphilus* in the leaves. However, the heatmap shows that also the inoculation via roots depleted the genus *Pseudomonas*, although the data were not statistically significant. In addition, *Pseudomonas* was the first represented genus in the rhizosphere with *Bacillus* and the second after *Bacillus* in the endorhizosphere. *Pseudomonas* accounted for 131 OTUs, four of which represented 91.8% of the reads in the rhizosphere, endorhizosphere, and xylem of sour orange inoculated and non-inoculated plants.

Only a few fungal genera were significantly differentially expressed and were more numerous in the rhizospheres than in the endorhizosphere, both in the leaf- and root-inoculated sour orange seedlings (Figure 4B, Supplementary Tables S8 and S9). *Plenodomus* was significantly enriched in the rhizosphere and endorhizosphere samples from root-inoculated seedlings (Figure 4B). In accordance with the increased relative abundance of Trichocomaceae in the rhizosphere of root-inoculated seedlings, the genus *Penicillium* was enriched. Other fungal genera, such as *Conlarium* and *Arthrotrichum* were also enriched, whereas *Pilidiella* was the only enriched genus in the leaf-inoculated ones (Supplementary Table S10). Interestingly, *Phialemonium* was depleted in each treatment both in the rhizosphere and endorhizosphere (Supplementary Tables S10 and S11). *Sterigmatomyces* in the root-inoculated and *Minimedusa*, *Rhizopus*, and *Umbelopsis* in the leaf-inoculated plants were all depleted. In the endorhizosphere, *Phialocephala* was enriched in both treatments. *Conlarium* and *Scytalidium* were enriched and depleted upon root-inoculation, respectively (Figure 4B). In xylem, *Minimedusa* (Supplementary Table S12) was the only significant taxon detected in the leaf-inoculated samples whereas no differentially abundant genera were detected in the root-inoculated samples (Supplemental Table S13).

### 3.2.5. *P. tracheiphilus* Infection Altered the Sour Orange Microbial Co-Occurrence Network

Infections caused by *P. tracheiphilus* upon wound penetration of the leaves greatly increased the number of nodes and edges in the network, compared to the network of the non-inoculated plants (89 vs. 141 nodes; 202 vs. 764 edges) (Table 1).

**Table 1.** Topological properties of control, leaf-inoculated, and root-inoculated plants co-occurrence networks.

Network	No. of Nodes	No. of Edges	Positive Edges	Percentage of Positive Edges (PEP)	Clustering Coefficient	Average Shortest Path	Modularity
Control	89	202	194	90.3%	0.166	3.027	0.415
Leaf-inoculated	141	764	686	81.9%	0.267	2.697	0.375
Root-inoculated	188	1315	1284	93.4%	0.292	2.724	0.286

In addition, the negative interactions increased in the leaf-inoculated plants, as revealed by a decrease in the positive edge percentage (PEP) (Table 1). Similarly, changes in the network of the microbial communities of the root-inoculated sour orange seedlings were characterized by an increase in the total nodes and edges, whose numbers were two and five times higher, respectively, in comparison to the nodes and edges in the control network. Moreover, in the presence of the pathogen, the networks of the microbial community in the leaf- and root-inoculated samples were more connected and less modularized than those of the control samples (Figure 5A–C).

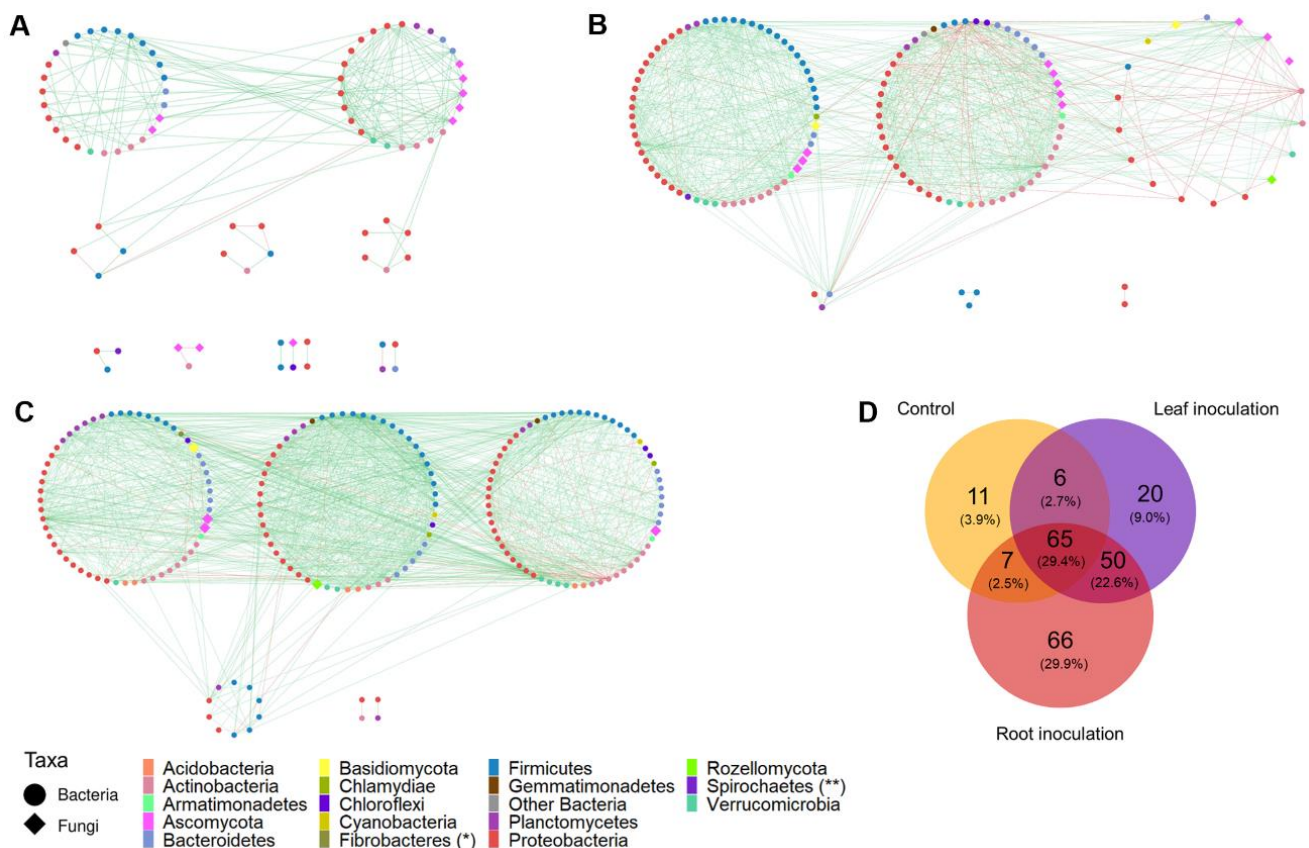


**Figure 5.** Co-occurrence networks of bacterial and fungal communities in control (A), leaf-inoculated (B), and root-inoculated (C) plants. The node and the edges represent microbial genera and the correlations among them, respectively. Each node is colored according to the phylum taxonomic level. (\*) Phylum only in the network of the root-inoculated plants. (\*\*) Phylum only in the network of the leaf-inoculated plants. (D) Venn diagram showing numbers of bacterial and fungal genera shared between the control samples and the leaf- and root-inoculated samples.

Comparing the nodes of the microbial community networks, 65 nodes were shared between the three networks, and 50 more nodes were shared between the networks of the inoculated samples, thus making a total of 115 nodes in common between the inoculated samples (Figure 5D).

The differential networks analysis showed that after the leaf- and root-inoculations with *P. tracheiphilus*, the microbial community structure underwent to a rewiring, therefore the nodes in common involved in the correlations between the leaf-inoculated and the root-inoculated samples networks were 7 and 14, respectively (Supplementary Tables S14 and S15). The networks of the inoculated samples showed that the microbial correlations in common were represented by 66 edges, involving 55 nodes (Supplementary Table S16) which represent around 48% of the 115 leaf- and root-inoculated samples' shared nodes.

#### 4. Discussion

Mal secco disease (MSD) is caused by the vascular fungus *P. tracheiphilus* and is the most detrimental disease in lemon trees [2]. There are currently no effective methods to control the disease. Where the disease is present, in order to contain infection it is essential to prune (and burn) withered shoots and remove suckers, which will then reduce inoculum [2–5,67]. Authorized fungicides (including copper-based) applications are recommended in the nursery or orchards, during the rainy season, after hailstorms, frost damage, and pruning. Currently, genotypes that combine resistance to *P. tracheiphilus* infection that have competitive yields or can be used on a large scale to control the disease in infected citrus-producing areas are not available. Many studies have been carried out to establish lemon cultivars that combine resistance to the disease with suitable agronomic and qualitative characteristics [68,69].

In this study, we determined whether the *P. tracheiphilus* infection alters the composition and interactions of microbial (bacterial and fungal) communities associated with the roots and xylem endosphere of sour orange, the most popular rootstock of lemon trees in Italy.

Since the pathogen enters the citrus above-ground organs and roots exclusively through wounds [3–5], natural MSD infections were simulated by leaf- and root-artificial inoculations.

The results obtained by quantitative real-time and by an amplicon-based (16S rRNA and ITS sequences) metagenomic approach showed that: (i) *P. tracheiphilus* colonized roots (upon root-inoculation) and xylem (upon leaf- and root-inoculation) of sour orange seedlings and was also detected by a metagenomic approach; (ii) *P. tracheiphilus* infections affected the communities of bacterial and fungal taxa with a potential role in biocontrol and (iii) rewired the microbial co-occurrence interactions in sour orange roots.

According to previous studies, the fungus can reach the leaves before they show disease symptoms by moving inside the vessels through passively transported conidia [4,8]. The fungus can then remain segregated in the inner wood layer for a short time or many years, determining a latent phase of the disease, until it reaches the most external woody rings and the disease progresses rapidly [3–5].

ITS amplicon-based metagenomic analysis of infected samples identified as *P. chrysanthemi* three OTUs phylogenetically related to *P. tracheiphilus* and *P. chrysanthemi* strains. These OTUs were not detected in the non-inoculated controls. The two *Plenodomus* species could not be differentiated from each other on the basis of their ITS sequences but can be pathogenic toward different hosts, such as *P. chrysanthemi* infects *Chrysanthemum* spp. while *P. tracheiphilus* rutaceous host plants [70,71]. In addition, results obtained by species-specific real-time PCR detection and absolute quantification of *P. tracheiphilus* suggest that the three OTUs identified as *P. chrysanthemi* belong to the inoculated *P. tracheiphilus* isolate.

Analysis of microbial communities of sour orange control seedlings showed a profile partially consistent with that observed in other *Citrus* studies [12]. The rhizosphere was characterized by the dominant presence of the bacterial phyla Proteobacteria, Firmicutes, and Planctomycetes, while Ascomycota and Basidiomycota were prevalent amongst fungal communities. Differences observed in comparison to previous observations are putatively due to our experimental conditions. Nearly all studies investigating the response of the citrus microbiome to biotic stresses were performed in open-field conditions with mature plants [26,28,29,33,34,36]. The endorhizosphere was dominated by Firmicutes

and Proteobacteria as also observed in other citrus pathosystems [26,29,37,72] and the xylem by Cyanobacteria, the third represented phylum, already observed in the citrus endorhizosphere [28]. At the fungal phylum level, Ascomycota and Basidiomycota were the most representative taxa in the endorhizosphere, in line with Yang and Ancona [28].

Regardless of the inoculation through leaves or roots, the differential abundance of the bacterial and fungal communities varied greatly in the infected plants. The genera *Pseudomonas* and *Burkholderia* were depleted in both leaf- and root-inoculated plants although more markedly in the rhizosphere of leaf-inoculated plants, while other citrus core bacterial taxa (e.g., *Streptomyces*) were increased in the endorhizosphere of plants inoculated both through the leaves and roots. The genus *Pseudomonas* belongs to the core member taxa of the citrus rhizosphere [11] and includes many biocontrol agents of plant pathogens [73]. Strains belonging to the *Pseudomonas fluorescens* complex have been efficiently used to mitigate MSD infection, as a result of the inhibition of spore germination and hyphal elongation of *P. tracheiphilus* during leaf and root penetration [4].

In line with our results, the populations of potentially beneficial *Pseudomonas* have decreased in other citrus pathosystems, particularly on foot rot [28], Citrus Decline Disease [26], and HLB infection [29]. The decrease in beneficial microbial taxa under foot rot infection has been proposed to enhance root decline by increasing susceptibility to environmental stress and colonization by phytopathogens [28]. Along with the genus *Pseudomonas*, *Burkholderia* belongs to the core member taxa of the citrus rhizosphere and possesses high rhizocompetence traits [11,74,75]. *Burkholderia* has been associated with uninfected citrus root samples [29,72] and reported as the dominant rhizosphere-to-rhizoplane enriched genus in HLB-infected citrus plants, encompassing species capable of combatting the growth of citrus pathogens by producing antimicrobial compounds and eliciting host defense responses [36,76,77]. Among the enriched genera, *Streptomyces* is a member of the core citrus bacterial community across compartments [11,30,33] and, in line with our results, was enriched in the citrus roots of HLB late symptomatic citrus trees, which thus suggested that it did not contribute to the mitigation of HLB disease symptoms [33]. By contrast, *Streptomyces* root endophytic populations were decreased in foot rot-diseased plants [28]. Members of this genus are natural antagonists of several fungal phytopathogens, comprising the xylematic pathogen *Verticillium* [78]. In the xylem endosphere, only a few bacterial and fungal taxa were either enriched or depleted. Of the enriched taxa, *Hydrogenophaga* was associated with high *Xylella fastidiosa* abundance in olive trees [79] and the mycoparasitic fungus *Minimedusa* has been reported in poplar plants affected by vascular wilt [80].

Among the fungal taxa, *Penicillium* was significantly enriched in the rhizosphere of root-inoculated plants. Including species recognized as postharvest pathogens of citrus fruits [81], *Penicillium* is one of the most abundant fungal genera associated with citrus roots [23]; in HLB-infected plants, the relative abundance of *Penicillium* was found to be either higher [32] or lower [36] compared to healthy plants. No information on arbuscular mycorrhizal fungi (AMF) was obtained in this study. A negative impact on their presence could be due to peat composition, nutrient levels, and microbiological properties [82,83]. AMF were shown to enhance citrus growth, nutrient and water acquisition, and, overall, resistance to abiotic stress conditions [84]. Populations of AMF belonging to the phylum Glomeromycota decreased in the roots of HLB- and foot rot-diseased citrus plants [33]. To gain insights into the multispecies microbial interactions involving *P. tracheiphilus*, co-occurrence networks were explored in the root environment upon root or leaf infections with the pathogen. The study revealed that regardless of the inoculation site (leaves or roots), the infection process intensified the microbial networks in the root environment. Notably, an increased negative interaction was observed under leaf-inoculation. According to previous studies, complex microbe–microbe interactions may contribute to counteracting the colonization of invading pathogens [85]. Pathogen-induced network-wide changes in microbial interactions have already been observed in different *Citrus* pathosystems and plant compartments. In the HLB pathosystem, in the leaves, the infection was found to determine negative interactions between CLAs and a few bacterial taxa of citrus core

microbiota [30]. Negative interactions among bacterial taxa also occurred under penicillin treatment conducted to reduce HLB disease severity [38]. Positive correlations between the abundance of CLAs and bacterial taxa in the roots and leaves have been reported less frequently [30,33,72,86]. With respect to other xylematic pathogens, the soil-borne fungus *Verticillium dahliae* was found to produce major changes in the topology of bacterial community networks of olive tree roots [87]. On the other hand, the bacterium *Xylella fastidiosa* revealed negative associations with different bacterial taxa in xylem-infected almond trees [88]. Changes in the microbial communities upon inoculation with *P. tracheiphilus*, even in plant compartments not colonized by the pathogen (as occurred in the leaf-inoculated plants), also suggest that these events may be mediated by the activation of the physiological responses of the sour orange host to the invading pathogen. Similarly, in citrus plants affected by HLB, physiological changes (e.g., a varied distribution of photosynthesis products) due to the leaf infection were found to restructure the native microbial community also in the rhizosphere, a compartment lacking direct competition with the phloem-limited bacterium '*Ca. Liberibacter asiaticus*' [29,89].

The observed microbiome variations could be therefore linked to physiological responses described in sour orange plants affected by MSD and associated with the extensive clogging of leaf veins, altering water transport inside the xylem vessels [9], with chloroplast damage and with the inhibition of the photosynthetic fixation of carbon due to the activity of malseccin complex of toxins [4,90]. The imposition of an oxidative stress status and a deep transcriptional reprogramming have also been reported in the infected leaves [91,92]. In addition, transcriptome analysis of *P. tracheiphilus* during the infection process revealed a multifaceted strategy to attack citrus hosts, involving the destruction of plant defensive metabolites and the optimization of fungus development and pathogenesis [93].

## 5. Conclusions

Citrus is an important tree crop worldwide, with Italy being a major producer in the Mediterranean Basin. The microbiome associated with citrus plays a decisive role in plant health by contributing to alleviating biotic and abiotic stresses. Among citrus diseases, Mal secco (MS) is caused by the vascular fungus *Plenodomus tracheiphilus* (*Pt*). The disease severely threatens the growth and productivity of citrus trees and no curative approaches have been developed to manage it.

To the best of our knowledge, this study provides for the first time the evidence of community-level changes in root- and xylem-associated microbes in response to *Pt* artificial inoculation (through leaves or roots) in sour orange, commonly used as rootstock for lemon trees in Italy. These changes mainly consist of the differential recruitment of core members of the citrus microbiome and in a network-wide rewiring of microbial inter-kingdom associations. Host physiological responses induced by the pathogen invasion are assumed to be the drivers of the microbial behavior observed. Further investigations on resident microbial communities under MSD pressure in the open field could be exploited for the selection of potentially citrus-beneficial microorganisms and the development of sustainable biocontrol products.

**Supplementary Materials:** The following supporting information can be downloaded at: <https://www.mdpi.com/article/10.3390/agronomy13030654/s1>, Figure S1: Alpha diversity estimations of the bacterial and fungal communities. Figure S2: PCoA biplot based on the Bray-Curtis dissimilarity index depicting (A) bacterial and (B) fungal communities beta diversity; Figure S3: Cladogram of *Plenodomus tracheiphilus* isolates and representative Pleosporales based on the partial ITS1 gene sequences; Table S1: Quantification of *Plenodomus tracheiphilus* DNA by real-time PCR and *Plenodomus* reads identified by ITS amplicons sequencing; Tables S2–S7: Bacterial differential abundance among the rhizosphere, endorhizosphere and xylem samples of control, leaf- and root-inoculated plants, respectively; Tables S8–S13: Fungal differential abundance among the rhizosphere, endorhizosphere and xylem samples of control, leaf- and root-inoculated plants, respectively; Tables S14–S16: Nodes sharing the same edges between the networks of control plants vs. leaf- and root-inoculated plants, respectively.

**Author Contributions:** Conceptualization, G.D., A.M. and V.C.; methodology, G.D., A.M., G.P., A.P. and V.C.; software, A.M., G.F.P. and A.P.; validation, A.P. and V.C.; formal analysis, G.D., A.M., D.N., A.A. and V.C.; investigation, G.D., A.M., G.P., D.N. and V.C.; resources, G.D., A.M. and V.C.; data curation, G.D., A.M. and V.C.; writing—original draft preparation, G.D., A.M. and V.C.; writing—review and editing, G.D., A.M., A.A., D.N. and V.C.; visualization, V.C.; supervision, A.P., V.C.; project administration, V.C.; funding acquisition, V.C. All authors have read and agreed to the published version of the manuscript.

**Funding:** This research work was funded by the project “Sviluppo di induttori di resistenza a patogeni vascolari degli agrumi” (S.I.R.P.A.) Misura 1.1.5 del PO FESR Sicilia 2014/2020. CUP: G68118000680007.

**Data Availability Statement:** The data presented in this study are available on request from the corresponding author.

**Conflicts of Interest:** The authors declare no conflict of interest.

## References

1. FAO. *Citrus Fruit Statistical Compendium 2020*; FAO: Rome, Italy, 2021.
2. EFSA PLH Panel. Scientific opinion on the pest categorisation of *Plenodomus tracheiphilus* (Petri) Gruyter, Aveskamp & Verkley [syn. *Phoma tracheiphila* (Petri) LA Kantschaveli & Gikashvili]. *EFSA J.* **2014**, *12*, 3775.
3. Migheli, Q.; Cacciola, S.O.; Balmas, V.; Pane, A.; Ezra, D.; Magnano di San Lio, G. Mal secco disease caused by *Phoma tracheiphila*: A potential threat to lemon production worldwide. *Plant Dis.* **2009**, *93*, 852–867. [[CrossRef](#)] [[PubMed](#)]
4. Nigro, F.; Ippolito, A.; Salerno, M.G. Mal secco disease of citrus: A journey through a century of research. *J. Plant Pathol.* **2011**, *93*, 523–560.
5. Catara, A.; Catara, V. Il “Mal Secco” Degli Agrumi, da un Secolo in Sicilia. In *Memorie e Rendiconti*; USPI Associato all’Unione Stampa Periodica Italiana: Giovanni Battista RM, Italy, 2019; Volume 3, pp. 35–58.
6. Krasnov, H.; Ezra, D.; Bahri, B.A.; Cacciola, S.O.; Meparishvili, G.; Migheli, Q.; Blank, L. Potential distribution of the citrus Mal Secco disease in the Mediterranean basin under current and future climate conditions. *Plant Pathol.* **2022**, 1–9. [[CrossRef](#)]
7. Perrotta, G.; Magnano di San Lio, G.; Lo Giudice, L.; Bassi, M. Ultrastructural modifications induced by *Phoma tracheiphila* in sour orange. *Riv. Di Patol. Veg.* **1979**, *14*, 25–33.
8. Bassi, M.; Magnano di San Lio, G.; Perrotta, G. Morphological observations on the host-parasite relations in sour orange leaves infected with *Phoma tracheiphila*. *J. Phytopathol.* **1980**, *98*, 320–330. [[CrossRef](#)]
9. Raimondo, F.; Raudino, F.; Cacciola, S.O.; Salleo, S.; Gullo, M.A.L. Impairment of leaf hydraulics in young plants of *Citrus aurantium* (sour orange) infected by *Phoma tracheiphila*. *Funct. Plant Biol.* **2007**, *34*, 720–729. [[CrossRef](#)]
10. Wang, N.; Stelinski, L.L.; Pelz-Stelinski, K.S.; Graham, J.H.; Zhang, Y. Tale of the Huanglongbing disease pyramid in the context of the citrus microbiome. *Phytopathology* **2017**, *107*, 380–387. [[CrossRef](#)]
11. Xu, J.; Zhang, Y.; Zhang, P.; Trivedi, P.; Riera, N.; Wang, Y.; Liu, X.; Fan, G.; Tang, J.; Coletta-Filho, H.D.; et al. The structure and function of the global citrus rhizosphere microbiome. *Nat. Commun.* **2018**, *9*, 4894. [[CrossRef](#)]
12. Zhang, Y.; Trivedi, P.; Xu, J.; Roper, M.C.; Wang, N. The citrus microbiome: From structure and function to microbiome engineering and beyond. *Phytobiomes J.* **2021**, *5*, 249–262. [[CrossRef](#)]
13. Vandenkoornhuyse, P.; Quaiser, A.; Duhamel, M.; Le Van, A.; Dufresne, A. The importance of the microbiome of the plant holobiont. *New Phytol.* **2015**, *206*, 1196–1206. [[CrossRef](#)] [[PubMed](#)]
14. Schlaeppi, K.; Spaepen, S.; van Themaat, E.V.L.; Schulze-Lefert, P. Structure and functions of the bacterial microbiota of plants. *Annu. Rev. Plant Biol.* **2013**, *64*, 807–838. [[CrossRef](#)]
15. Lombardi, N.; Woo, S.L.; Vinale, F.; Turrà, D.; Marra, R. Editorial: The plant holobiont volume II: Impacts of the rhizosphere on plant health. *Front. Plant Sci.* **2021**, *12*, 809291. [[CrossRef](#)] [[PubMed](#)]
16. Raaijmakers, J.M.; Paulitz, T.; Steinberg, C.; Alabouvette, C.; Moëgne-Loccoz, Y. The rhizosphere: A playground and battlefield for soilborne pathogens and beneficial microorganisms. *Plant Soil* **2008**, *321*, 341–361. [[CrossRef](#)]
17. Berg, G.; Rybakova, D.; Fischer, D.; Cernava, T.; Vergès, M.-C.C.; Charles, T.; Chen, X.; Cocolin, L.; Eversole, K.; Corral, G.H.; et al. Microbiome definition re-visited: Old concepts and new challenges. *Microbiome* **2020**, *8*, 103. [[CrossRef](#)] [[PubMed](#)]
18. Liu, Y.-X.; Qin, Y.; Chen, T.; Lu, M.; Qian, X.; Guo, X.; Bai, Y. A practical guide to amplicon and metagenomic analysis of microbiome data. *Protein Cell* **2020**, *12*, 315–330. [[CrossRef](#)]
19. Berendsen, R.L.; Pieterse, C.M.J.; Bakker, P.A.H.M. The rhizosphere microbiome and plant health. *Trends Plant Sci.* **2012**, *17*, 478–486. [[CrossRef](#)]
20. Mendes, R.; Garbeva, P.; Raaijmakers, J.M. The rhizosphere microbiome: Significance of plant beneficial, plant pathogenic, and human pathogenic microorganisms. *FEMS Microbiol. Rev.* **2013**, *37*, 634–663. [[CrossRef](#)]
21. Compant, S.; Samad, A.; Faist, H.; Sessitsch, A. A review on the plant microbiome: Ecology, functions, and emerging trends in microbial application. *J. Adv. Res.* **2019**, *19*, 29–37. [[CrossRef](#)]



22. Faddetta, T.; Abbate, L.; Alibrandi, P.; Arancio, W.; Siino, D.; Strati, F.; De Filippo, C.; Del Bosco, S.F.; Carimi, F.; Puglia, A.M.; et al. The endophytic microbiota of *Citrus limon* is transmitted from seed to shoot highlighting differences of bacterial and fungal community structures. *Sci. Rep.* **2021**, *11*, 7078. [[CrossRef](#)]
23. Blacutt, A.; Ginnan, N.; Dang, T.; Bodaghi, S.; Vidalakis, G.; Ruegger, P.; Peacock, B.; Viravathana, P.; Vieira, F.C.; Drozd, C. An in vitro pipeline for screening and selection of citrus-associated microbiota with potential anti-“*Candidatus Liberibacter asiaticus*” properties. *Appl. Environ. Microbiol.* **2020**, *86*, e02883-19. [[CrossRef](#)]
24. Penyalver, R.; Roesch, L.F.; Piquer-Salcedo, J.E.; Forner-Giner, M.A.; Alguacil, M.D.M. From the bacterial citrus microbiome to the selection of potentially host-beneficial microbes. *New Biotechnol.* **2022**, *70*, 116–128. [[CrossRef](#)] [[PubMed](#)]
25. Li, P.-D.; Zhu, Z.-R.; Zhang, Y.; Xu, J.; Wang, H.; Wang, Z.; Li, H. The phyllosphere microbiome shifts toward combating melanose pathogen. *Microbiome* **2022**, *10*, 56. [[CrossRef](#)] [[PubMed](#)]
26. Passera, A.; Alizadeh, H.; Azadvar, M.; Quaglino, F.; Alizadeh, A.; Casati, P.; Bianco, P.A. Studies of Microbiota dynamics reveals association of “*Candidatus Liberibacter Asiaticus*” Infection with Citrus (*Citrus sinensis*) decline in South of Iran. *Int. J. Mol. Sci.* **2018**, *19*, 1817. [[CrossRef](#)]
27. Abdelfattah, A.; Cacciola, S.O.; Mosca, S.; Zappia, R.; Schena, L. Analysis of the fungal diversity in citrus leaves with greasy spot disease symptoms. *Microb. Ecol.* **2016**, *73*, 739–749. [[CrossRef](#)] [[PubMed](#)]
28. Yang, C.; Ancona, V. Metagenomic analysis reveals reduced beneficial microorganism associations in roots of foot-rot-affected citrus trees. *Phytobiomes J.* **2021**, *5*, 305–315. [[CrossRef](#)]
29. Trivedi, P.; He, Z.; Van Nostrand, J.; Albrigo, G.; Zhou, J.; Wang, N. Huanglongbing alters the structure and functional diversity of microbial communities associated with citrus rhizosphere. *ISME J.* **2011**, *6*, 363–383. [[CrossRef](#)]
30. Blaustein, R.A.; Lorca, G.L.; Meyer, J.L.; Gonzalez, C.F.; Teplitski, M. Defining the core citrus leaf- and root-associated microbiota: Factors associated with community structure and implications for managing huanglongbing (Citrus Greening) disease. *Appl. Environ. Microbiol.* **2017**, *83*, e00210-17. [[CrossRef](#)]
31. Wang, N.; Pierson, E.A.; Setubal, J.C.; Xu, J.; Levy, J.G.; Zhang, Y.; Li, J.; Rangel, L.T.; Martins, J., Jr. The *Candidatus liberibacter*-host interface: Insights into pathogenesis mechanisms and disease control. *Annu. Rev. Phytopathol.* **2017**, *55*, 451–482. [[CrossRef](#)]
32. Padhi, E.M.T.; Maharaj, N.; Lin, S.-Y.; Mishchuk, D.O.; Chin, E.; Godfrey, K.; Foster, E.; Polek, M.; Leveau, J.H.J.; Slupsky, C.M. Metabolome and microbiome signatures in the roots of citrus affected by huanglongbing. *Phytopathology* **2019**, *109*, 2022–2032. [[CrossRef](#)]
33. Ginnan, N.A.; Dang, T.; Bodaghi, S.; Ruegger, P.M.; McCollum, G.; England, G.; Vidalakis, G.; Borneman, J.; Rolshausen, P.E.; Roper, M.C. Disease-induced microbial shifts in citrus indicate microbiome-derived responses to huanglongbing across the disease severity spectrum. *Phytobiomes J.* **2020**, *4*, 375–387. [[CrossRef](#)]
34. Li, H.; Song, F.; Wu, X.; Deng, C.; Xu, Q.; Peng, S.; Pan, Z. Microbiome and Metagenome analysis reveals huanglongbing affects the abundance of citrus rhizosphere bacteria associated with resistance and energy metabolism. *Horticulturae* **2021**, *7*, 151. [[CrossRef](#)]
35. Munir, S.; Li, Y.; He, P.; Huang, M.; He, P.; He, P.; Cui, W.; Wu, Y.; He, Y. Core endophyte communities of different citrus varieties from citrus growing regions in China. *Sci. Rep.* **2020**, *10*, 3648. [[CrossRef](#)]
36. Zhang, Y.; Xu, J.; Riera, N.; Jin, T.; Li, J.; Wang, N. Huanglongbing impairs the rhizosphere-to-rhizoplane enrichment process of the citrus root-associated microbiome. *Microbiome* **2017**, *5*, 97. [[CrossRef](#)] [[PubMed](#)]
37. Bai, Y.; Wang, J.; Jin, L.; Zhan, Z.; Guan, L.; Zheng, G.; Qiu, D.; Qiu, X. Deciphering bacterial community variation during soil and leaf treatments with biologicals and biofertilizers to control huanglongbing in citrus trees. *J. Phytopathol.* **2019**, *167*, 686–694. [[CrossRef](#)]
38. Ascunce, M.S.; Shin, K.; Huguet-Tapia, J.C.; Poudel, R.; Garrett, K.A.; van Bruggen, A.H.C.; Goss, E.M. Penicillin trunk injection affects bacterial community structure in citrus trees. *Microb. Ecol.* **2018**, *78*, 457–469. [[CrossRef](#)]
39. Yang, C.; Powell, C.A.; Duan, Y.; Shatters, R.; Fang, J.; Zhang, M. Deciphering the bacterial microbiome in huanglongbing-affected citrus treated with thermotherapy and sulfonamide antibiotics. *PLoS ONE* **2016**, *11*, e0155472. [[CrossRef](#)]
40. Zhang, M.; Powell, C.A.; Benyon, L.S.; Zhou, H.; Duan, Y. Deciphering the bacterial microbiome of citrus plants in response to ‘*Candidatus liberibacter asiaticus*’-infection and antibiotic treatments. *PLoS ONE* **2013**, *8*, e76331. [[CrossRef](#)]
41. Lacava, P.; Araujo, W.; Marcon, J.; Maccheroni, W.; Azevedo, J. Interaction between endophytic bacteria from citrus plants and the phytopathogenic bacteria *Xylella fastidiosa*, causal agent of citrus-variegated chlorosis. *Lett. Appl. Microbiol.* **2004**, *39*, 55–59. [[CrossRef](#)]
42. Grasso, F.M.; Catara, V. Preliminary characterization of *Phoma tracheiphila* isolates from Italy and Greece by DNA-based typing methods. *J. Plant Pathol.* **2006**, *88*, S45.
43. Oliveri, C.; Modica, G.; Bella, P.; Dimaria, G.; Cirvilleri, G.; Continella, A.; Catara, V. Preliminary evaluation of a zinc-copper-citric acid biocomplex for the control of *Plenodomus tracheiphilus* causal agent of citrus mal secco disease. *Acta Hort.* **2022**, *1354*, 231–236. [[CrossRef](#)]
44. EPPO. PM 7/048 3 *Plenodomus tracheiphilus* (formerly *Phoma tracheiphila*). *EPPO Bull.* **2015**, *45*, 183–192.
45. Salerno, M.; Catara, A. Ricerche sul “mal secco” degli Agrumi (*Deuterophoma tracheiphila* Petri). VI. Indagini sulla riproduzione sperimentale della malattia. *Riv. Patol. Veg.* **1967**, *3*, 89–97.
46. Luisi, N.; De Cicco, V.; De Cico, V.; Cutuli, G.; Salerno, M. Ricerche su un metodo di studio della patogenicità del fungo del Mal secco degli Agrumi. *Ann. Dell’istituto Sper. Per L’agrumicoltura Di Acireale* **1979**, *9–10*, 167–173.

47. Scaramuzzi, G.; Salerno, M.; Catara, A. Ricerche sul Mal Secco degli agrumi (*Deuterophoma tracheiphila* Petri): II—Influenza delle basse temperature sul decorso della malattia. *Riv. Patol. Veg.* **1964**, *4*, 319–327.
48. Anzalone, A.; Di Guardo, M.; Bella, P.; Ghadamgahi, F.; Dimaria, G.; Zago, R.; Cirvilleri, G.; Catara, V. Bioprospecting of beneficial bacteria traits associated with tomato root in greenhouse environment reveals that sampling sites impact more than the root compartment. *Front. Plant Sci.* **2021**, *12*, 637582. [[CrossRef](#)]
49. Anzalone, A.; Mosca, A.; Dimaria, G.; Nicotra, D.; Tessitori, M.; Privitera, G.F.; Pulvirenti, A.; Leonardi, C.; Catara, V. Soil and soilless tomato cultivation promote different microbial communities that provide new models for future crop interventions. *Int. J. Mol. Sci.* **2022**, *23*, 8820. [[CrossRef](#)]
50. Licciardello, G.; Grasso, F.M.; Bella, P.; Cirvilleri, G.; Grimaldi, V.; Catara, V. Identification and detection of *Phoma tracheiphila*, causal agent of citrus mal secco disease, by real-time polymerase chain reaction. *Plant Dis.* **2006**, *90*, 1523–1530. [[CrossRef](#)]
51. Russo, M.; Grasso, F.; Bella, P.; Licciardello, G.; Catara, A.; Catara, V. Molecular diagnostic tools for the detection and characterization of *Phoma tracheiphila*. *Acta Hort.* **2011**, *892*, 207–214. [[CrossRef](#)]
52. Klindworth, A.; Pruesse, E.; Schweer, T.; Peplies, J.; Quast, C.; Horn, M.; Glöckner, F.O. Evaluation of general 16S ribosomal RNA gene PCR primers for classical and next-generation sequencing-based diversity studies. *Nucleic Acids Res.* **2013**, *41*, e1. [[CrossRef](#)]
53. White, T.J.; Bruns, T.; Lee, S.; Taylor, J. Amplification and direct sequencing of fungal ribosomal RNA genes for phylogenetics. In *PCR Protocols: A Guide to Methods and Applications*; Innis, M.A., Gelfand, D.H., Sninsky, J.J., White, T.J., Eds.; Academic Press: San Diego, CA, USA, 1990; pp. 315–322.
54. Andrews, S. FastQC: A Quality Control Tool for High Throughput Sequence Data. 2010. Available online: <https://www.bioinformatics.babraham.ac.uk/projects/fastqc/> (accessed on 4 July 2022).
55. Bolyen, E.; Rideout, J.R.; Dillon, M.R.; Bokulich, N.A.; Abnet, C.C.; Al-Ghalith, G.A.; Alexander, H.; Alm, E.J.; Arumugam, M.; Asnicar, F.; et al. Reproducible, interactive, scalable and extensible microbiome data science using QIIME 2. *Nat. Biotechnol.* **2019**, *37*, 852–857. [[CrossRef](#)] [[PubMed](#)]
56. Cole, J.R.; Wang, Q.; Fish, J.A.; Chai, B.; McGarrell, D.M.; Sun, Y.; Brown, C.T.; Porras-Alfaro, A.; Kuske, C.R.; Tiedje, J.M. Ribosomal database project: Data and tools for high throughput rRNA analysis. *Nucleic Acids Res.* **2014**, *42*, D633–D642. [[CrossRef](#)] [[PubMed](#)]
57. McDonald, D.; Price, M.N.; Goodrich, J.; Nawrocki, E.P.; DeSantis, T.Z.; Probst, A.; Andersen, G.L.; Knight, R.; Hugenholtz, P. An improved greengenes taxonomy with explicit ranks for ecological and evolutionary analyses of bacteria and archaea. *ISME J.* **2012**, *6*, 610–618. [[CrossRef](#)] [[PubMed](#)]
58. Kõljalg, U.; Nilsson, R.H.; Abarenkov, K.; Tedersoo, L.; Taylor, A.F.S.; Bahram, M.; Bates, S.T.; Bruns, T.D.; Bengtsson-Palme, J.; Callaghan, T.M.; et al. Towards a unified paradigm for sequence-based identification of fungi. *Mol. Ecol.* **2013**, *22*, 5271–5277. [[CrossRef](#)] [[PubMed](#)]
59. McMurdie, P.J.; Holmes, S. Phyloseq: An R package for reproducible interactive analysis and graphics of microbiome census data. *PLoS ONE* **2013**, *8*, e61217. [[CrossRef](#)] [[PubMed](#)]
60. R Core Team. *R: A Language and Environment for Statistical Computing*; R Foundation for Statistical Computing: Vienna, Austria, 2022.
61. Love, M.I.; Huber, W.; Anders, S. Moderated estimation of fold change and dispersion for RNA-seq data with DESeq2. *Genome Biol.* **2014**, *15*, 550. [[CrossRef](#)]
62. Deng, Y.; Jiang, Y.-H.; Yang, Y.; He, Z.; Luo, F.; Zhou, J. Molecular ecological network analyses. *BMC Bioinform.* **2012**, *13*, 113. [[CrossRef](#)]
63. Shannon, P.; Markiel, A.; Ozier, O.; Baliga, N.S.; Wang, J.T.; Ramage, D.; Amin, N.; Schwikowski, B.; Ideker, T. Cytoscape: A software environment for integrated models of Biomolecular Interaction Networks. *Genome Res.* **2003**, *13*, 2498–2504. [[CrossRef](#)]
64. Van Landeghem, S.; Van Parys, T.; Dubois, M.; Inzé, D.; Van de Peer, Y. Diffany: An ontology-driven framework to infer, visualise and analyse differential molecular networks. *BMC Bioinform.* **2016**, *17*, 18. [[CrossRef](#)]
65. Kumar, S.; Stecher, G.; Li, M.; Nnyaz, C.; Tamura, K. MEGA X: Molecular evolutionary genetics analysis across computing platforms. *Mol. Biol. Evol.* **2018**, *35*, 1547–1549. [[CrossRef](#)]
66. Kimura, M. A simple method for estimating evolutionary rates of base substitutions through comparative studies of nucleotide sequences. *J. Mol. Evol.* **1980**, *16*, 111–120. [[CrossRef](#)] [[PubMed](#)]
67. Batuman, O.; Ritenour, M.; Vicent, A.; Li, H.; Hyun, J.-W.; Catara, V.; Ma, H.; Cano, L.M. Chapter 17— Diseases caused by fungi and oomycetes. In *The Genus Citrus*, 1st ed.; Talon, M., Caruso, M., Gmitter, F.G., Eds.; Woodhead Publishing: Cambridge, UK, 2020; pp. 349–369. ISBN 978-0-12-812163-4.
68. Russo, R.; Caruso, M.; Arlotta, C.; Lo Piero, A.R.; Nicolosi, E.; Di Silvestro, S. Identification of field tolerance and resistance to mal secco disease in a citrus germplasm collection in Sicily. *Agronomy* **2020**, *10*, 1806. [[CrossRef](#)]
69. Catalano, C.; Di Guardo, M.; Distefano, G.; Caruso, M.; Nicolosi, E.; Deng, Z.; Gentile, A.; La Malfa, S.G. Biotechnological approaches for genetic improvement of lemon (*Citrus limon* (L.) burm. f.) against mal secco disease. *Plants* **2021**, *10*, 1002. [[CrossRef](#)] [[PubMed](#)]
70. Baker, K.F.; Davis, L.H.; Wilhelm, S.; Snyder, W.C. An aggressive vascular-inhabiting *Phoma* (*Phoma tracheiphila* f. sp. *chrysanthemi* nov. f. sp.) weakly pathogenic to chrysanthemum. *Can. J. Bot.* **1985**, *63*, 1730–1735. [[CrossRef](#)]
71. De Gruyter, J.; Woudenberg, J.H.C.; Aveskamp, M.M.; Verkley, G.J.M.; Groenewald, J.Z.; Crous, P.W. Redisposition of *Phoma*-like anamorphs in Pleosporales. *Stud. Mycol.* **2013**, *75*, 1–36. [[CrossRef](#)]

72. Trivedi, P.; Duan, Y.; Wang, N. Huanglongbing, a systemic disease, restructures the bacterial community associated with citrus roots. *Appl. Environ. Microbiol.* **2010**, *76*, 3427–3436. [\[CrossRef\]](#)
73. Bonaterra, A.; Badosa, E.; Daranas, N.; Francés, J.; Roselló, G.; Montesinos, E. Bacteria as biological control agents of plant diseases. *Microorganisms* **2022**, *10*, 1759. [\[CrossRef\]](#)
74. Lugtenberg, B.J.J.; Dekkers, L.; Bloemberg, G.V. Molecular determinants of rhizosphere colonization by *Pseudomonas*. *Annu. Rev. Phytopathol.* **2001**, *39*, 461–490. [\[CrossRef\]](#)
75. Berg, G.; Krechel, A.; Ditz, M.; Sikora, R.A.; Ulrich, A.; Hallmann, J. Endophytic and ectophytic potato-associated bacterial communities differ in structure and antagonistic function against plant pathogenic fungi. *FEMS Microbiol. Ecol.* **2005**, *51*, 215–229. [\[CrossRef\]](#)
76. Riera, N.; Handique, U.; Zhang, Y.; Dewdney, M.M.; Wang, N. Characterization of antimicrobial-producing beneficial bacteria isolated from huanglongbing escape citrus trees. *Front. Microbiol.* **2017**, *8*, 2415. [\[CrossRef\]](#)
77. Riera, N.; Wang, H.; Li, Y.; Li, J.; Pelz-Stelinski, K.; Wang, N. Induced systemic resistance against citrus canker disease by rhizobacteria. *Phytopathology* **2018**, *108*, 1038–1045. [\[CrossRef\]](#) [\[PubMed\]](#)
78. Carlucci, A.; Raimondo, M.L.; Colucci, D.; Lops, F. *Streptomyces albidoflavus* Strain CARA17 as a biocontrol agent against fungal soil-borne pathogens of fennel plants. *Plants* **2022**, *11*, 1420. [\[CrossRef\]](#) [\[PubMed\]](#)
79. Giampetruzzi, A.; Baptista, P.; Morelli, M.; Cameirão, C.; Neto, T.L.; Costa, D.; D’Attoma, G.; Kubaa, R.A.; Altamura, G.; Saponari, M.; et al. Differences in the endophytic microbiome of olive cultivars infected by *Xylella Fastidiosa* across seasons. *Pathogens* **2020**, *9*, 723. [\[CrossRef\]](#) [\[PubMed\]](#)
80. Kwaśna, H.; Szewczyk, W.; Baranowska, M.; Gallas, E.; Wiśniewska, M.; Behnke-Borowczyk, J. Mycobiota associated with the vascular wilt of poplar. *Plants* **2021**, *10*, 892. [\[CrossRef\]](#)
81. Wang, Z.; Sui, Y.; Li, J.; Tian, X.; Wang, Q. Biological control of postharvest fungal decays in citrus: A review. *Crit. Rev. Food Sci. Nutr.* **2020**, *62*, 861–870. [\[CrossRef\]](#)
82. Linderman, R.; Davis, E. Soil amendment with different peatmosses Affects mycorrhizae of onion. *Horttechnology* **2003**, *13*, 285–289. [\[CrossRef\]](#)
83. Vestberg, M.; Saari, K.; Kukkonen, S.; Hurme, T. Mycotrophy of crops in rotation and soil amendment with peat influence the abundance and effectiveness of indigenous arbuscular mycorrhizal fungi in field soil. *Mycorrhiza* **2005**, *15*, 447–458. [\[CrossRef\]](#)
84. Ortas, I. Chapter 23—Mycorrhiza in citrus: Growth and nutrition. In *Advances in citrus nutrition*; Srivastava, A.K., Ed.; Springer: Dordrecht, The Netherlands, 2012; pp. 333–351. ISBN 9789400741713.
85. Wei, Z.; Yang, T.; Friman, V.-P.; Xu, Y.; Shen, Q.; Jousset, A. Trophic network architecture of root-associated bacterial communities determines pathogen invasion and plant health. *Nat. Commun.* **2015**, *6*, 8413. [\[CrossRef\]](#)
86. Sagaram, U.S.; DeAngelis, K.M.; Trivedi, P.; Andersen, G.L.; Lu, S.-E.; Wang, N. Bacterial diversity analysis of huanglongbing pathogen-infected citrus, using phylochip arrays and 16S rRNA gene clone library sequencing. *Appl. Environ. Microbiol.* **2009**, *75*, 1566–1574. [\[CrossRef\]](#)
87. Fernández-González, A.J.; Cardoni, M.; Cabanás, C.G.-L.; Valverde-Corredor, A.; Villadas, P.J.; Fernández-López, M.; Mercado-Blanco, J. Linking belowground microbial network changes to different tolerance level towards *Verticillium* wilt of olive. *Microbiome* **2020**, *8*, 1–19. [\[CrossRef\]](#)
88. Anguita-Maeso, M.; Ares-Yebra, A.; Haro, C.; Román-Écija, M.; Olivares-García, C.; Costa, J.; Marco-Noales, E.; Ferrer, A.; Navas-Cortés, J.A.; Landa, B.B. *Xylella fastidiosa* infection reshapes microbial composition and network associations in the xylem of almond trees. *Front. Microbiol.* **2022**, *13*, 866085. [\[CrossRef\]](#) [\[PubMed\]](#)
89. Wang, N.; Trivedi, P. Citrus huanglongbing: A newly relevant disease presents unprecedented challenges. *Phytopathology* **2013**, *103*, 652–665. [\[CrossRef\]](#) [\[PubMed\]](#)
90. Fogliano, V.; Marchese, A.; Scaloni, A.; Ritieni, A.; Visconti, A.; Randazzo, G.; Graniti, A. Characterization of a 60 kDa phytotoxic glycoprotein produced by *Phoma tracheiphila* and its relation to malseccin. *Physiol. Mol. Plant Pathol.* **1998**, *53*, 149–161. [\[CrossRef\]](#)
91. Russo, R.; Sicilia, A.; Caruso, M.; Arlotta, C.; Di Silvestro, S.; Gmitter, F.G.; Nicolosi, E.; Lo Piero, A.R. De novo transcriptome sequencing of rough lemon leaves (*Citrus jambhiri* Lush.) in response to *Plenodomus tracheiphilus* infection. *Int. J. Mol. Sci.* **2021**, *22*, 882. [\[CrossRef\]](#)
92. Reverberi, M.; Betti, C.; Fabbri, A.A.; Zjalic, S.; Spadoni, S.; Mattei, B.; Fanelli, C. A role for oxidative stress in the *Citrus limon*/*Phoma tracheiphila* interaction. *Plant Pathol.* **2007**, *57*, 92–102. [\[CrossRef\]](#)
93. Sicilia, A.; Russo, R.; Caruso, M.; Arlotta, C.; Di Silvestro, S.; Gmitter, F.G.; Gentile, A.; Nicolosi, E.; Lo Piero, A.R. Transcriptome analysis of *Plenodomus tracheiphilus* infecting rough lemon (*Citrus jambhiri* Lush.) indicates a multifaceted strategy during host pathogenesis. *Biology* **2022**, *11*, 761. [\[CrossRef\]](#)

**Disclaimer/Publisher’s Note:** The statements, opinions and data contained in all publications are solely those of the individual author(s) and contributor(s) and not of MDPI and/or the editor(s). MDPI and/or the editor(s) disclaim responsibility for any injury to people or property resulting from any ideas, methods, instructions or products referred to in the content.